
Description and performance of the new baseline ESS moderators

	Name	Affiliation
Author	Luca Zanini	ESS TD
Reviewers	Ferenc Mezei Konstantin Batkov	ESS ESS TD
Approver	Eric Pitcher	ESS TD

Abstract

The design and expected neutronic performance of the new, updated baseline ESS moderators is presented.

DRAFT

1 Introduction

This document is intended as an accompanying document of the report [1] which contains a general description of the moderators' performance, including a presentation of the new McStas component: `ESS_butterfly.comp`, following the recent change of the focal points.

In the present document I present in more detail the design of the moderators, the MCNP model, and show the expected performance for all the ESS beam ports.

The ESS beam extraction layout (shown in Fig. 1 and Fig. 2) contains 42 beam ports, arranged in two sectors covering an angle of $2 \times 120^\circ$, all pointing to the center of the monolith where the thermal and cold moderators are placed. Two moderator systems were designed, one placed above, one below the target, with similar design, the main difference being the height of the moderators (3 cm for the top, 6 cm for the bottom). This report describes the top moderator only. The required minimum viewed surface area for neutron extraction is of 3 (height) \times 6 (width) cm^2 for both thermal and cold top moderators. The thermal and cold moderators are distinct moderators containing different materials (light water and 20 K parahydrogen, respectively). Moderators should be placed above the *hot spot* of neutron production, which is an area of approximately $15 \times 20 \text{ cm}^2$ (see Fig. 3) where most of the evaporation neutrons are emitted from the target in the spallation process. The moderator closer to the hot spot will be the brightest, and ideally both thermal or cold moderators should be placed on it.

Butterfly moderators [2, 3] are the design solution to provide bright bi-spectral moderators for the whole instrument suite. The need of bi-spectral extraction, and therefore the need to place, if possible, both thermal and cold moderators above the hot spot of neutron production, suggested the use of moderator shapes, such as shown in Fig. 4, which have the following advantages:

- Both cold and thermal moderators are placed on the hot spot, providing high thermal and cold brightness for a required extraction area of at least 3 (height) \times 6 (width) cm^2 for both thermal and cold moderators. The actual maximum viewed widths at the moderators, for all the beam ports are listed in Table 1.
- Such moderators are ideally fit for beam extraction in the two 120° sectors; the brightness variation across the sectors is within 10%.
- Their relatively compact shape is an advantage for beam extraction: for all the 42 beam ports, the thermal and cold extraction surfaces lie next to each other, being placed on the two sides of the focal points, allowing instruments to see the brightest part of thermal and cold moderators.
- Both thermal and cold moderator have a height of 3-cm for increased brightness [4].
- To some extent, and as much as it is possible for the wide extraction area, also the concept of tube moderators [5] is exploited, because of the presence of straight walls corresponding to the cold neutron extraction, adjacent to thermal premoderators. This is particularly true for some beam lines, and will give additional gain in beam extraction areas narrower than 6 cm are used, as shown later in this report.

2 Focal points

The focal points are the points in the absolute coordinate system, to which the axes of the beam ports are pointed. They are the origin of the beamport axes. They are defined in the

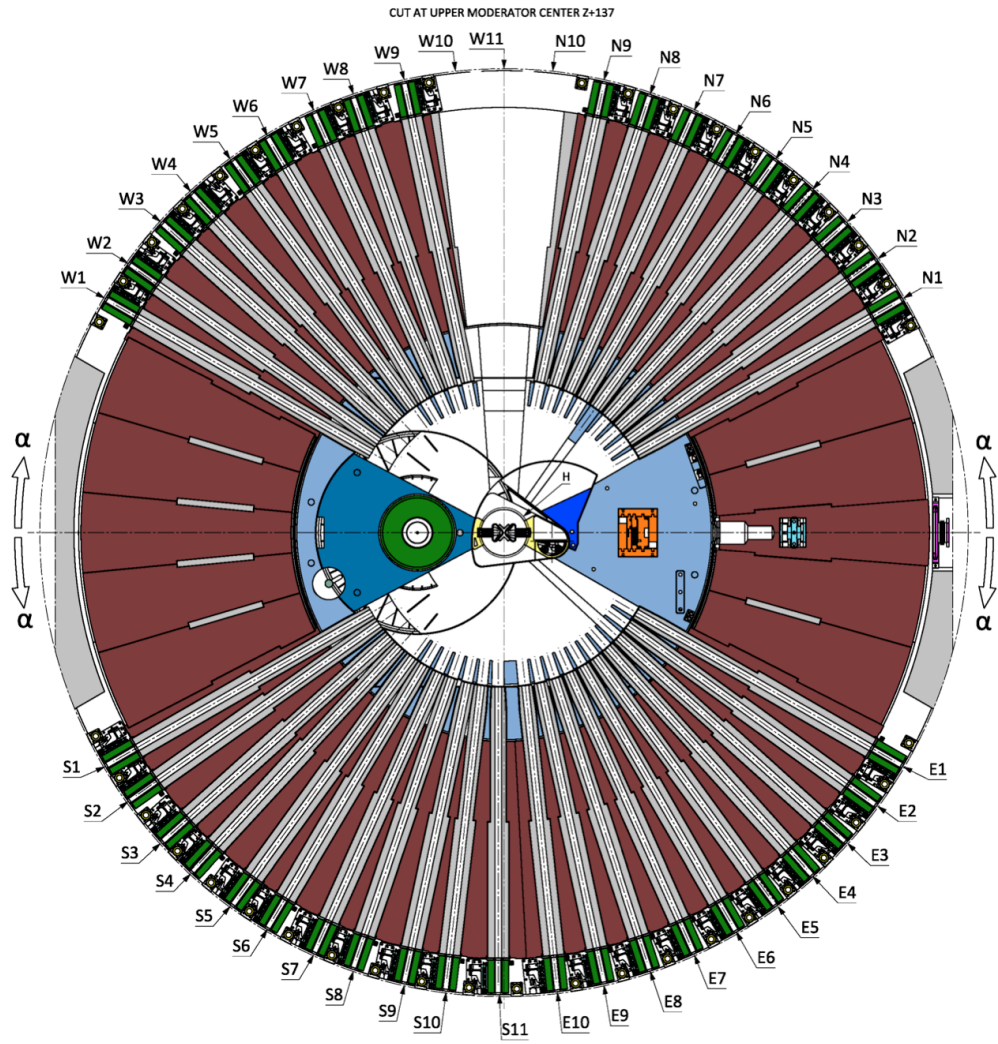


Figure 1: Horizontal section cut of the monolith structures, at the level of the upper moderator position above the target wheel. Proton beam comes from the right. The moderators are placed in the center. Neutron beam extraction optics start at 2 m and extend out to 5.5 m in the form of inserts (grey) installed horizontally into the beam ports (brown). Shutters (green) fill the space from 5.5 m to 6 m.

Target Coordinate System (TCS), in which the origin is the point with vertical coordinate being at the center of the target, and with the two horizontal coordinates being at the center of the moderators (Fig. 5).

The shape of the moderator and the focal points coordinates are strongly linked: the moderator shape (and in particular the transition between thermal and cold moderator) defines the focal point position, because the focal points are between the surface for thermal and cold neutron extraction. Beam guides are oriented to look at a thermal or cold emitting surface, and their orientation is related to the focal point position.

The focal points are different for the four instrument sectors: the previous focal points for the North sector are $X=75$ mm, $Y=89$ mm, $Z=137$ mm). For the other sectors, the absolute values of the X and Y coordinates are unchanged, but the signs change according to

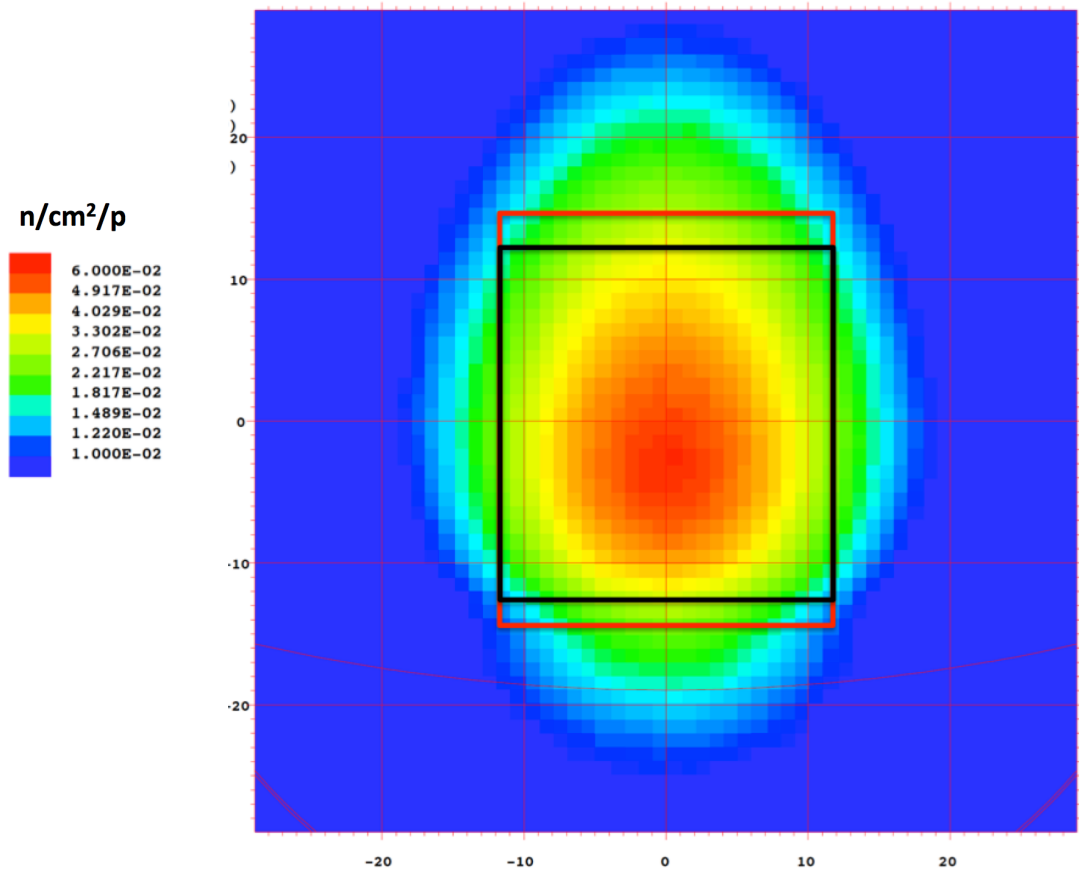


Figure 3: Maps of high-energy ($E > 0.1$ MeV) neutrons crossing a plane located between the tungsten target and the premoderator. The red and black squares indicate the extension of the current and changed positions of the cold moderators, respectively. (The proton beam direction in the figure is upwards.) Reduction of extension in the lateral direction will increase the shadow effect of monolith structures.

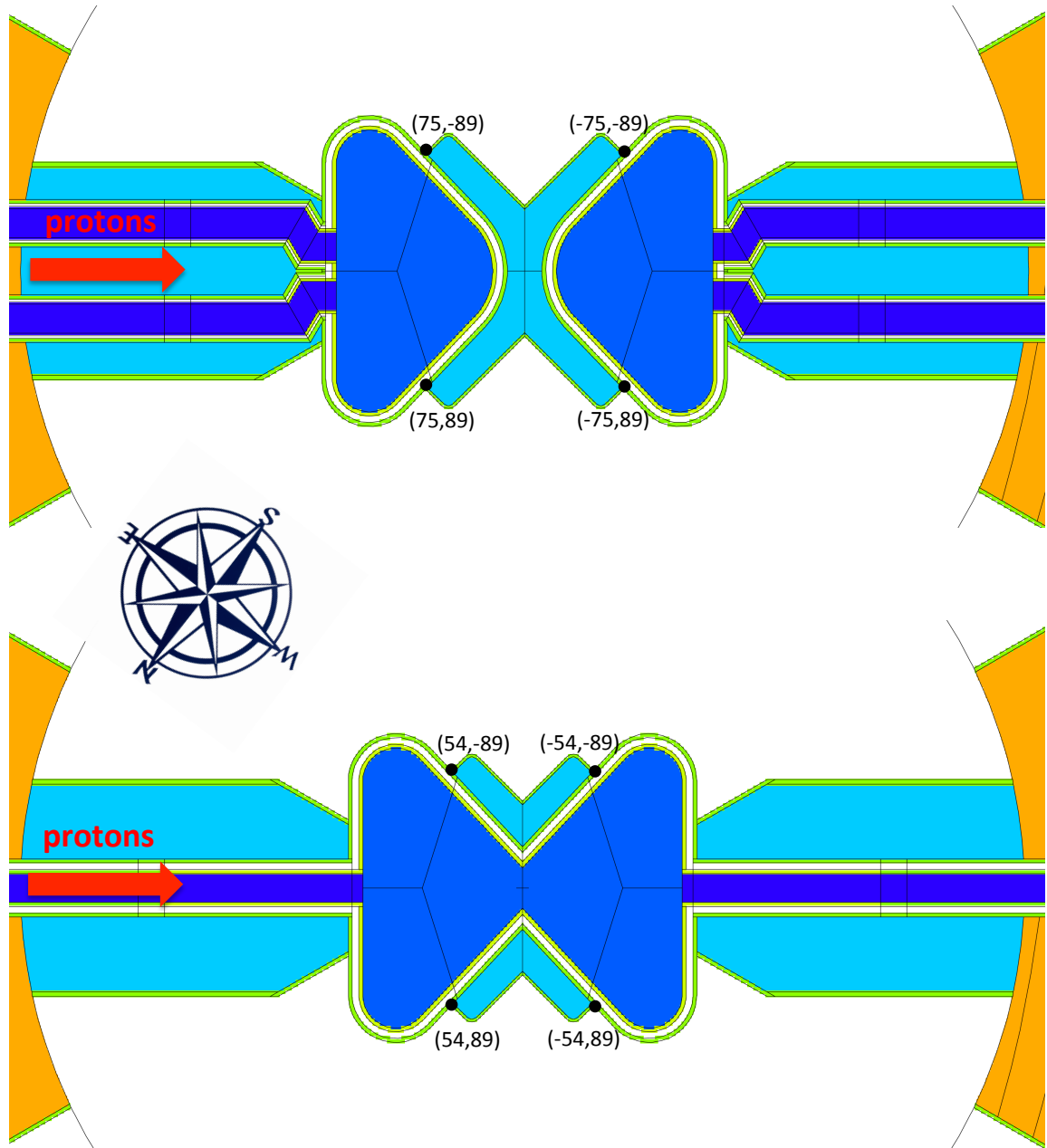


Figure 4: MCNPX models of the two butterfly designs. *Top*: BF2 design, where the cold moderator is split in two parts, and the water moderator occupies a major part of the hot spot *Bottom*: BF1 design, with a single cold moderator vessel and light water moderators, all placed above the neutron production hot spot. The focal points, the origin of the beamport inserts, are indicated. The new official focal points are the ones in the figure at the bottom. Since the design has essentially been shrunk in the direction of the proton beam, the Y value is the same in the two designs, while the X value is different, being closer to each other by 42 mm in the BF1 design. The red arrows indicate the direction of the incoming proton beam, impinging on the tungsten target located below the moderator.

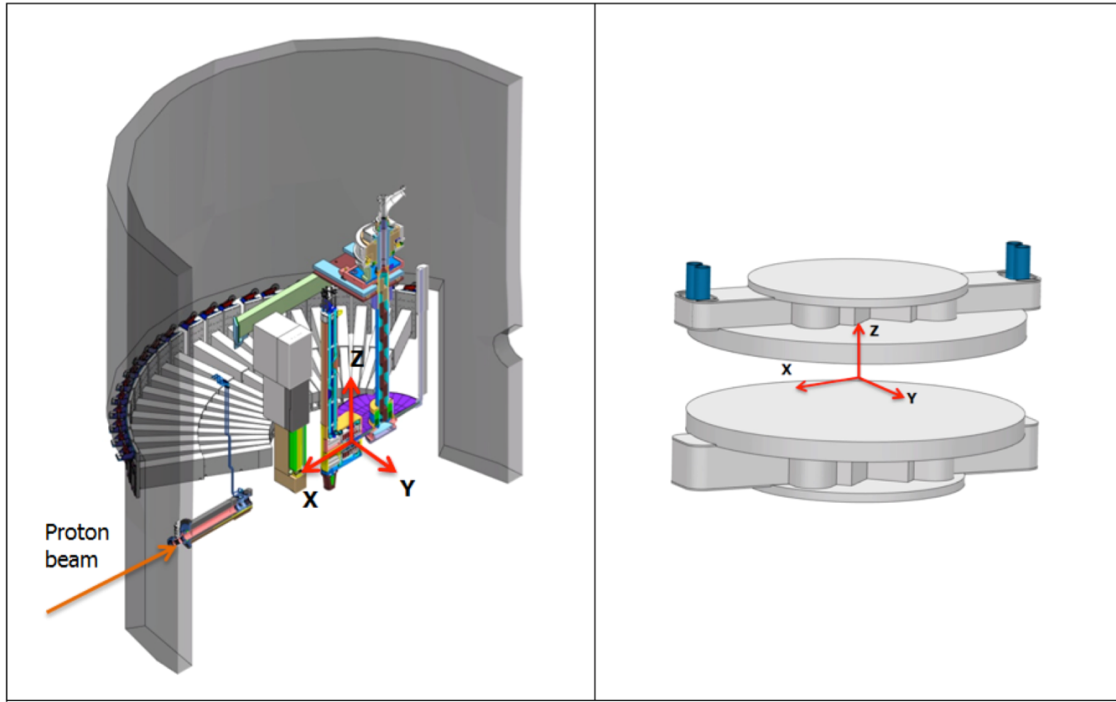


Figure 5: The Target Coordinate System (TCS).

the sector (see Fig. 4)).

The new focal points are (for the North sector) $X=54$ mm, $Y=89$ mm, $Z=137$ mm. The reasons for the change are explained in detail in Ref. [1]. There are clear advantages in terms of improved cold neutron performance, without loss in thermal brightness. The horizontal view width (see next paragraph) for the cold moderator is increased for some of the beam lines. Furthermore, in the BF2 design the horizontal view width of the thermal moderator was considerably larger (up to 15 cm) than the cold one, in contrast with the fact that most ESS instruments are cold or bi-spectral, and therefore there should be a better balance of the horizontal view widths.

3 Description of the MCNP model

The geometry of the butterfly moderator with the new focal points is shown in Fig. 6. Engineering details have been extrapolated from the existing engineering model of the BF2 design.

The MCNPX model is shown in Figs. 6 to 9. Some important details of the model are the following:

- MCNPX, version 2.7.0 [10, 11] was used, with the default Bertini/Dresner spallation/evaporation models and ENDF-VII neutron libraries.
- The tungsten target was modeled according to the engineering drawings. The density of the tungsten used in the model is of 15.1 g/cm^3 , corresponding to the effective density deduced from the engineering design, which consists of tungsten bricks with cooling gaps, for a filling factor of tungsten of 78%. The target is shown in detail in Fig. 9. The SS316L container of the bricks was modeled in detail according to the engineering drawings.

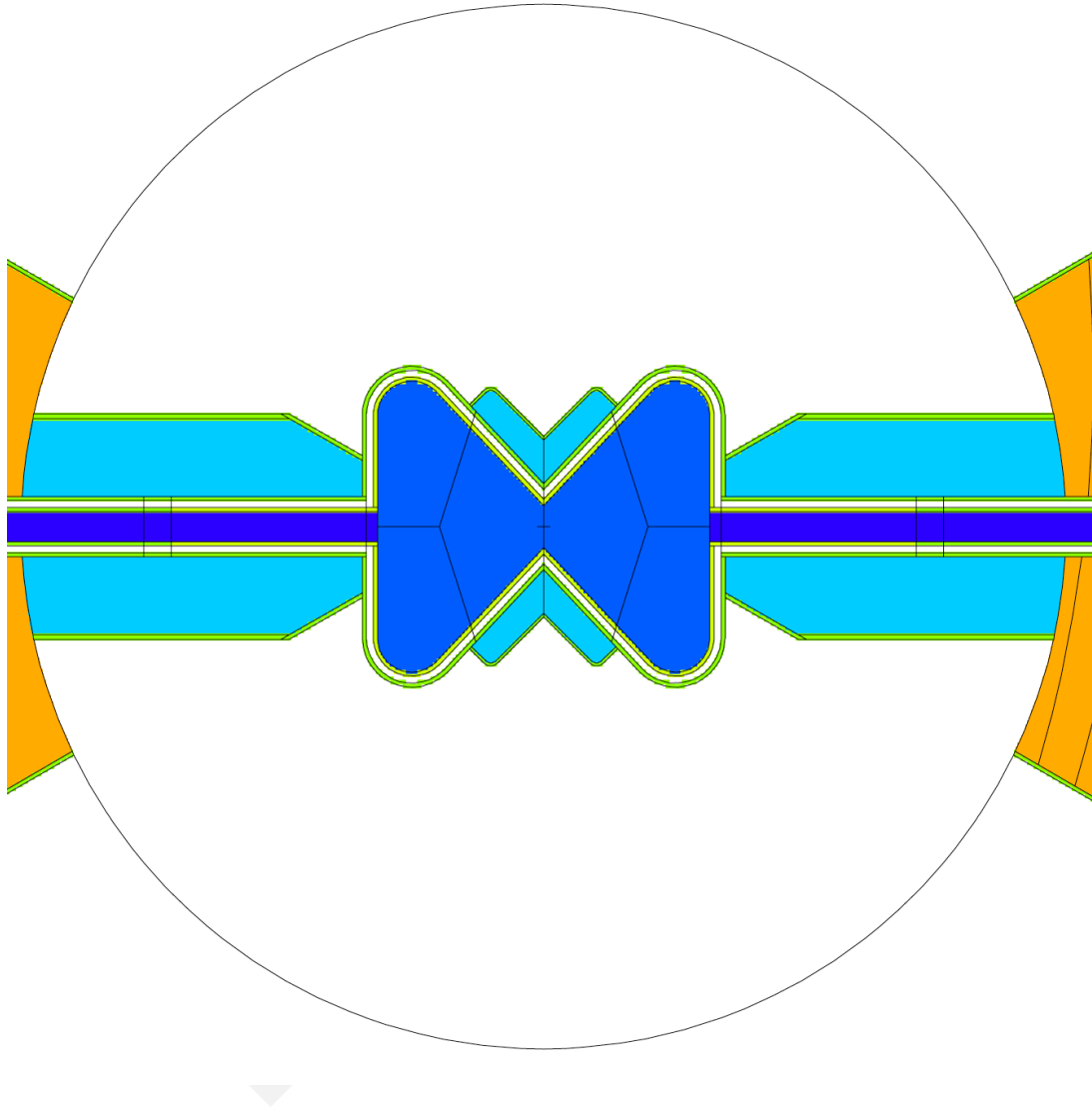


Figure 6: MCNPX geometry of the moderator, top view. The proton beam comes from the left. The parahydrogen contains 5 vol% of Al in the model, to account for the presence of Al flow channels, not yet designed. On the sides of the cold moderator, inlet and outlet hydrogen pipes, including vacuum gaps, are modeled. Water is placed around the pipes to serve as premoderator and increase the brightness of the cold moderator.

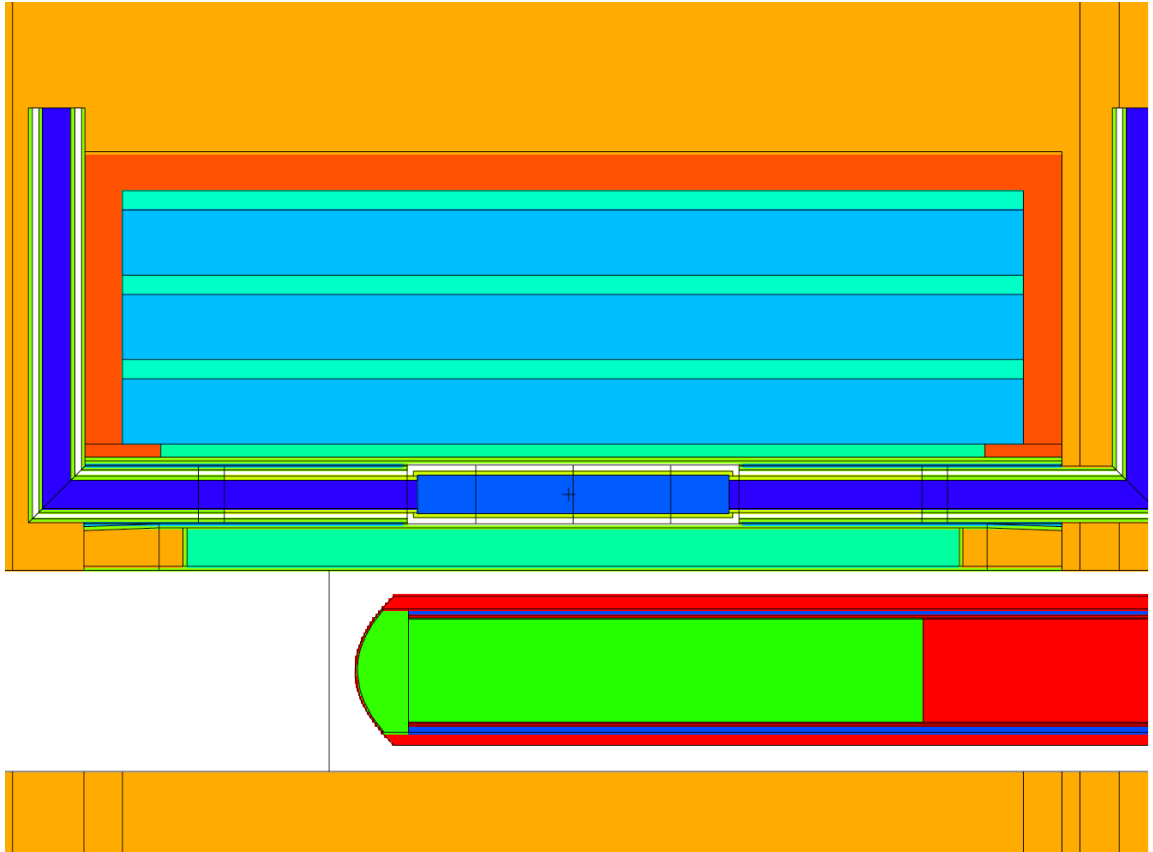


Figure 7: MCNPX geometry used for the brightness calculations, side view. Proton beam comes from the left impinging on the tungsten target. Tungsten (green) has a density of 15.1 g/cm^3 instead of the nominal density of 19.3 g/cm^3 to account for the fraction of helium in the target according to which the filling factor of tungsten is 78 vol%. The water premoderator (green) between target and moderator has a 8% volume fraction of Al, to account for flow channels. The beryllium reflector (light blue) includes water channels (green) according to engineering drawings. The reflector is contained in stainless steel (red). The outer reflector (orange) is made of stainless steel, with 10% volume fraction of water, for cooling.

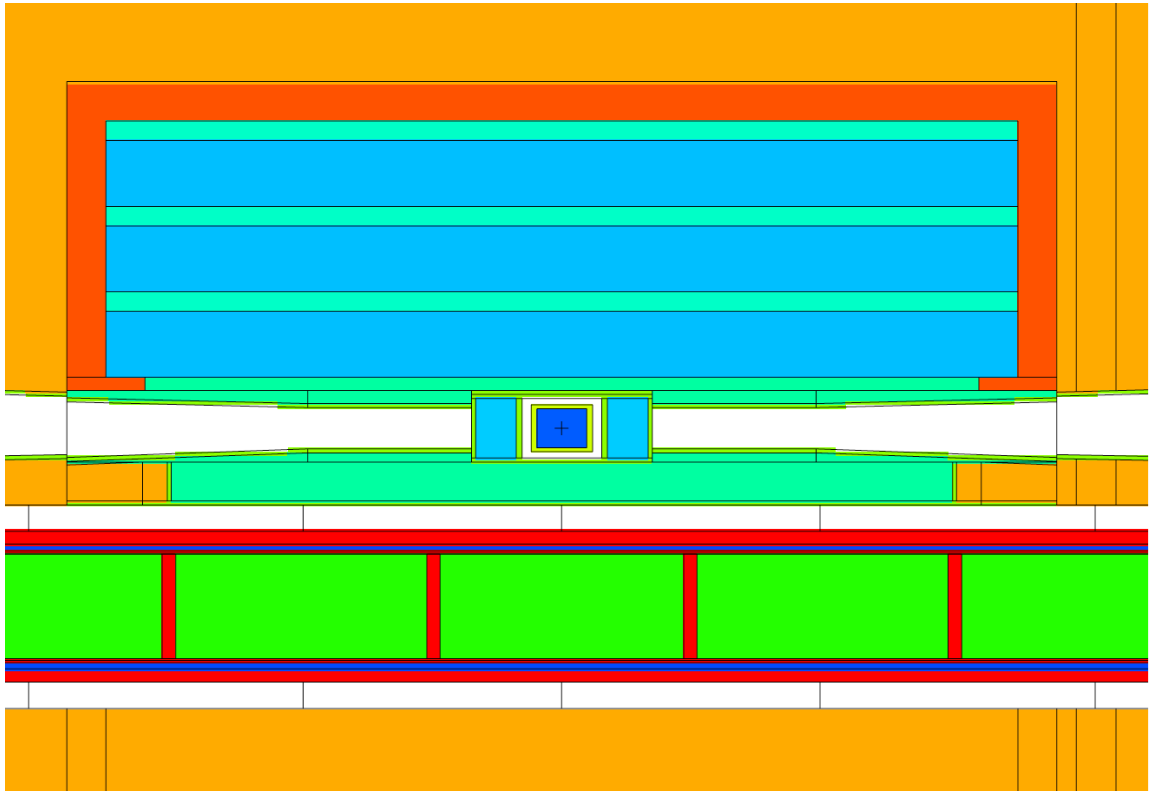


Figure 8: MCNPX geometry used for the brightness calculations, side view showing beam extraction channels. The proton beam is entering the figure.

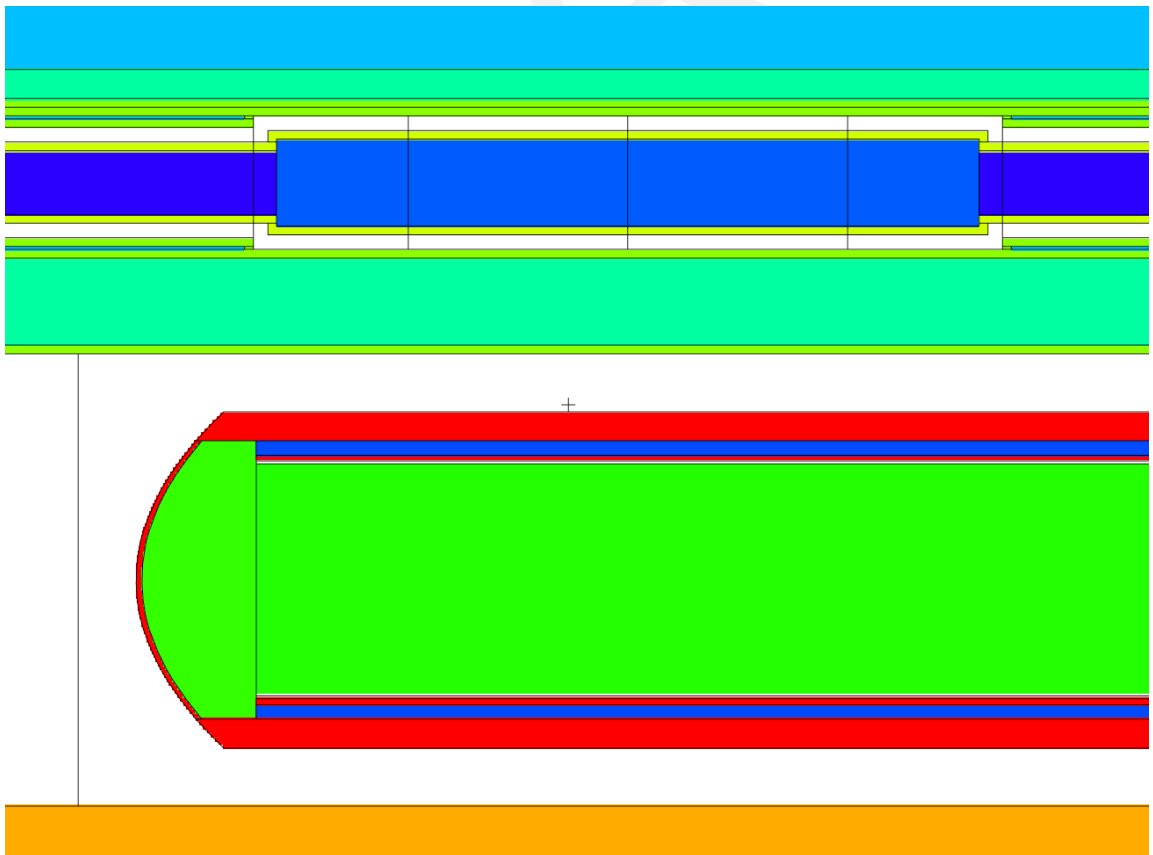


Figure 9: MCNPX geometry used for the brightness calculations, side view, showing details of the target. The front part of the target is shown with the same green colour of the tungsten, but the material is He.

- The water premoderator between target and moderator consists of an Al vessel, containing a mixture of water and aluminum, with a volume fraction of Al of 8 vol%, deduced from the engineering drawings of the water premoderator currently in construction.
- Similarly, parahydrogen in the cold moderator contains 5 vol% of Al, corresponding to the expected volume fraction occupied by the flow channels. The shape and thickness of the Al vessel is modeled according to the engineering drawings.
- the parahydrogen ENDF-VII cross section was used. However, according to recent precise measurement of the parahydrogen cross section [12], the ENDF-VII cross section measurement was not performed on pure parahydrogen, but on a sample which had a fraction of 0.5% of orthohydrogen. Therefore, we set pure parahydrogen in the material composition, thus accounting for a 0.5% impurity of orthohydrogen, which is the upper limit aimed at during operation.
- Thicknesses of Al walls of the cold, thermal moderators, and of the Be reflector are in agreement with the engineering drawings.
- Design changes accepted in 2015 of the target design and target-moderator distance have been implemented in the model.
- The Be reflector is modeled according to the present status of the engineering design, with the expected amount of light water cooling.
- The outer reflector is made of SS316L with 10 vol% of water cooling.
- Two pipes, inlet and outlet, are assumed for the cold moderator, see Figs. 6 and 7.
- The top 3 cm BF1 moderator is modeled. At the bottom, a block of SS316L (with 10 vol% of water) is placed in the model.

3.1 Horizontal view width

Fig. 10 shows the maximum horizontal viewed width at the moderator surface, for thermal and cold moderators, for the different beam ports. The widths for the beam ports N1, W1, S1, and E1 are limited by the monolith structures. As noted in Ref. [1], there is now a much better balance between maximum widths of thermal and cold moderators, with respect to the previous design, which had much larger widths for the thermal moderators and significantly smaller widths for the cold moderators.

4 Moderator performance

4.1 Wavelength spectra

Fig. 11 shows the peak wavelength spectra, averaged over the 42 beam ports. The peak brightness is the brightness within the ESS long pulse, i.e., the average brightness multiplied by 25 (the inverse of the duty factor $1/(14 \text{ Hz} \times 2.867 \cdot 10^{-3} \text{ sec})$). The procedure for the brightness calculation is explained in Appendix A. As shown in the following subsection, there is some variation of absolute brightness with the beam port angle. However, the shapes of the thermal and cold spectra are the same for all the beam ports.

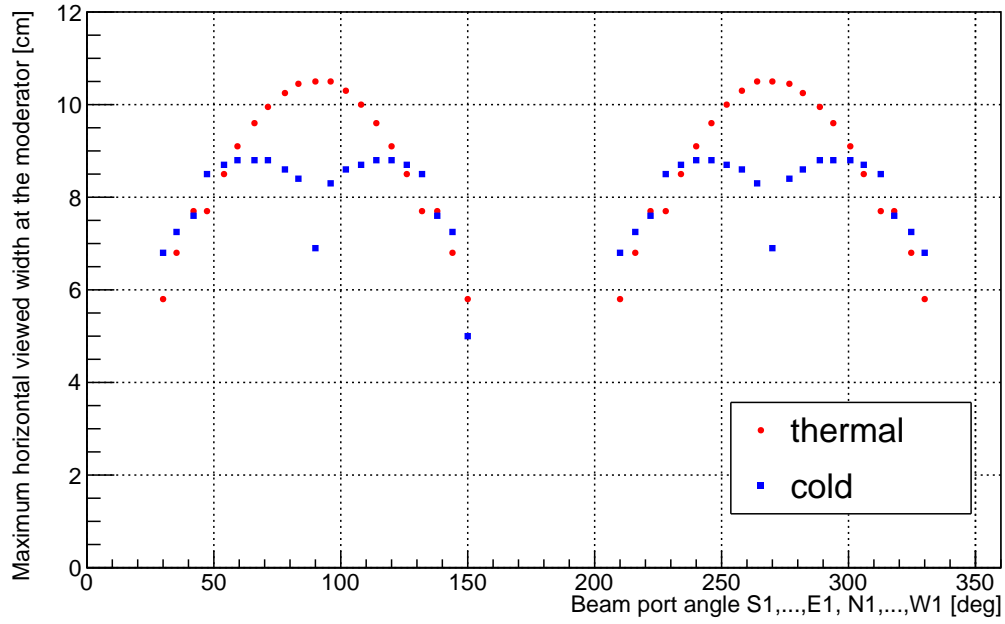


Figure 10: Horizontal maximum view at the thermal and cold moderator surface for the different beam ports. See explanation in the text. For correspondence between angle and beam port see Table 1.

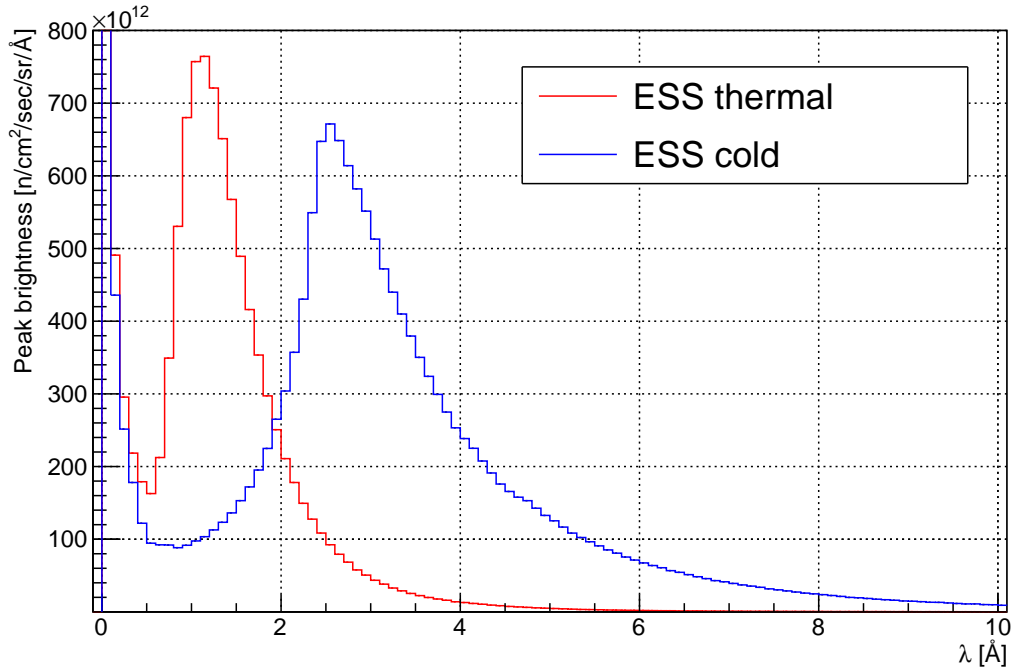


Figure 11: Thermal and cold peak wavelength spectra, for 6-cm wide extraction at the moderator, averaged over the 42 beam ports.

Table 1: Maximum viewed width at the thermal and cold moderators for the 42 beam ports. For W11 and S11 the cold width can be doubled, if cold neutrons are extracted from both side of the butterfly moderator. For N1, W1, S1 and E1 the maximum cold width is limited by the structure of the monolith. Uncertainties of 1 mm should be considered for the widths. The angles in the second column are a convention used in this report: from Fig. 2, angles are counted from the direction of the proton beam, counterclockwise, so that S1 is at 30°, E1 at 150°, N1 at 210°, and W1 at 330°.

beam port	angle [degrees]	cold width [cm]	thermal width [cm]
S 1	30	6.8	5.8
S 2	35.3	7.25	6.8
S 3	42	7.6	7.7
S 4	47.3	8.5	7.7
S 5	54	8.7	8.5
S 6	59.3	8.8	9.1
S 7	66	8.8	9.6
S 8	71.3	8.8	9.95
S 9	78	8.6	10.25
S 10	83.3	8.4	10.45
S 11	90	6.9	10.5
E 10	96	8.3	10.5
E 9	102	8.6	10.3
E 8	108	8.7	10
E 7	114	8.8	9.6
E 6	120	8.8	9.1
E 5	126	8.7	8.5
E 4	132	8.5	7.7
E 3	138	7.6	7.7
E 2	144	7.25	6.8
E 1	150	5	5.8
N 1	210	6.8	5.8
N 2	216	7.25	6.8
N 3	222	7.6	7.7
N 4	228	8.5	7.7
N 5	234	8.7	8.5
N 6	240	8.8	9.1
N 7	246	8.8	9.6
N 8	252	8.7	10
N 9	258	8.6	10.3
N 10	264	8.3	10.5
W 11	270	6.9	10.5
W 10	276.7	8.4	10.45
W 9	282	8.6	10.25
W 8	288.7	8.8	9.95
W 7	294	8.8	9.6
W 6	300.7	8.8	9.1
W 5	306	8.7	8.5
W 4	312.7	8.5	7.7
W 3	318	7.6	7.7
W 2	324.7	7.25	6.8
W 1	330	6.8	5.8

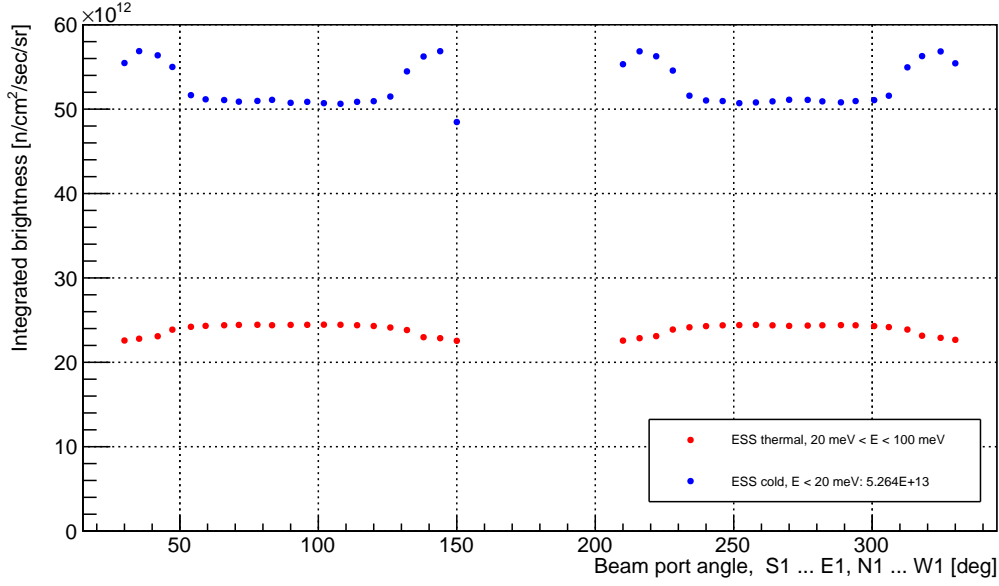


Figure 12: Time average integrated thermal and cold brightness for the 42 beam ports. Thermal brightness integrated between 20 meV and 100 meV. Cold brightness integrated between 0 and 20 meV. For correspondence between angle and beam port see Table 1. Note the drop in brightness for the E1 beam port at 150°; in this calculation it was assumed a 5 cm width due to known interference with the twister mechanism that holds the moderator-reflector plug. However, according to recent information from the engineering teams, this problem can be solved and E1 will have the same maximum horizontal view width and brightness of N1.

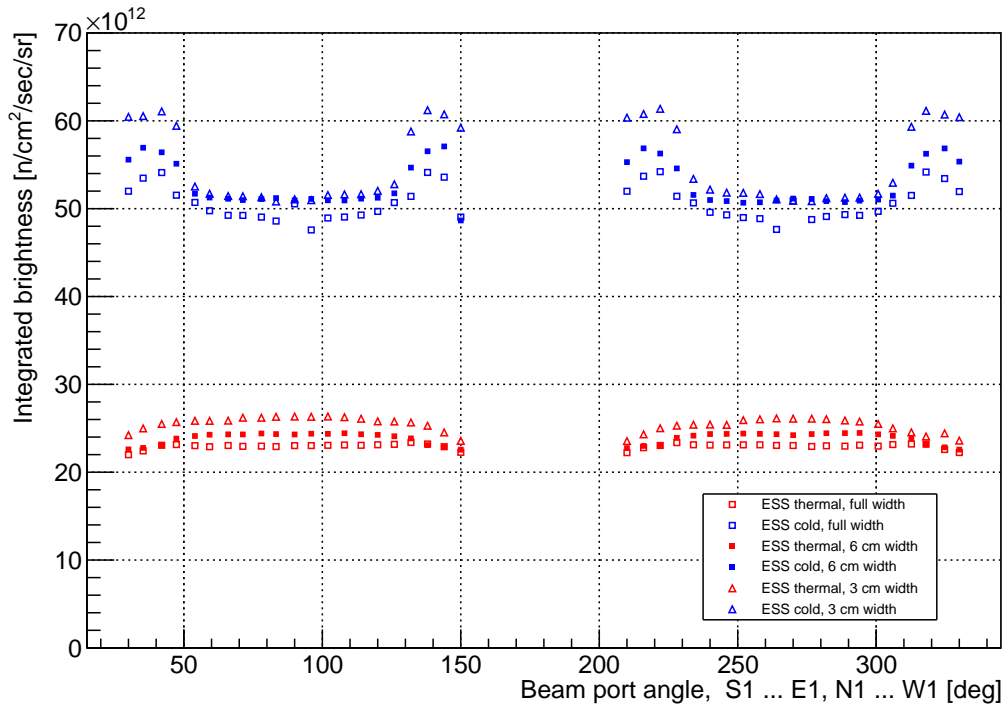


Figure 13: Time average integrated thermal and cold brightness for the 42 beam ports. Thermal brightness integrated between 20 meV and 100 meV. Cold brightness integrated between 0 and 20 meV. See explanation in the text. For correspondence between angle and beam port see Table 1.

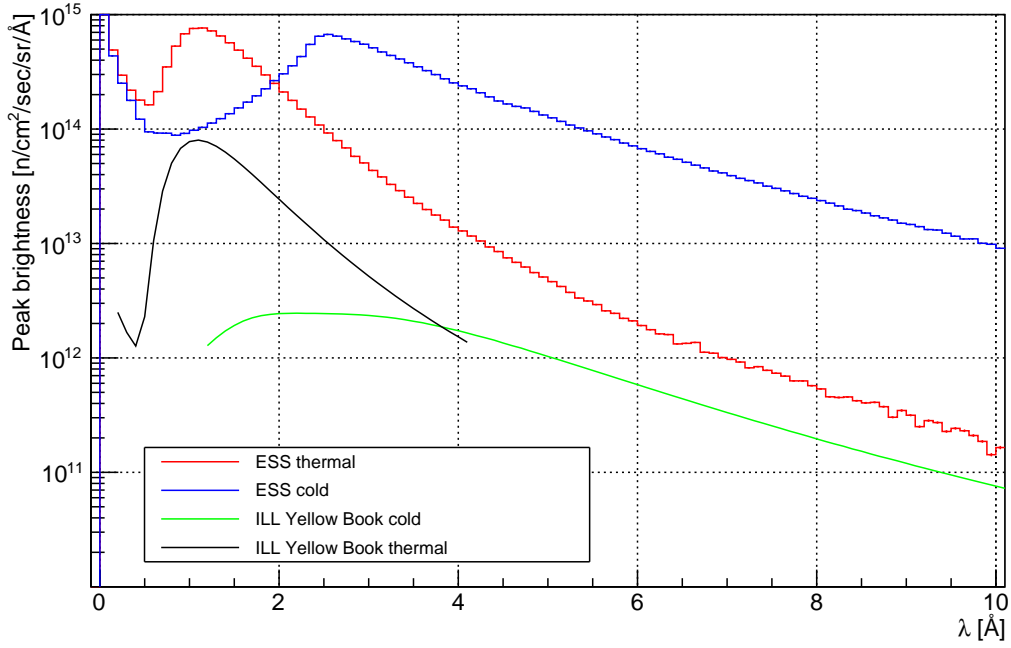


Figure 14: Brightness spectra averaged over 42 beam ports for 3 cm high moderator, compared with ILL official curves[8].

4.2 Performance of the individual beam ports

Fig. 12 shows the integrated time-averaged brightness distribution along the 42 ESS beam ports, calculated for a horizontal viewed width at the moderator of 6 cm. Fig. 13 contains additional information:

- results for the 6 cm viewed widths;
- brightness calculated viewing the maximum width at the moderator (the values of maximum width per beam port are given in Fig. 10 and Table 1). The brightness looking to the maximum width is a bit smaller than the brightness for 6-cm width, as expected.
- Additionally, brightness curves are calculated for an extraction width of 3 cm. In this case the extraction position at the moderator surface is optimized to give the maximum brightness. This gives a clear brightness increase, which is particularly relevant for those cold beam lines, for which it is possible to exploit the full length of the cold moderator.

4.3 Absolute uncertainty

The present design is an extrapolation from the engineering model of the BF2 design. All the engineering details are described in the paragraph “Description of the MCNP model”. The engineering design of the BF1, and in particular the flow channels, is not performed yet, but an attempt to include all the engineering details (and associated penalties in neutron production) is made in agreement with the information available from the existing design, as described in the paragraph.

To quote absolute uncertainties on the brightness values one must also consider the uncertainties related to the Monte Carlo calculation. MCNPX calculations are based on spallation/evaporation models, and on nuclear libraries (available mostly up to 150 MeV energy), which includes also the scattering kernels. A detailed study of uncertainties related to these

contributions was done for a previous baseline change [13]. On the basis of those results, and considering the more mature level of the present design, we can expect an absolute uncertainty of 15% on the present brightness values.

4.4 Comparison to previous ESS designs and to ILL

Before the introduction of low-dimensional moderators, the reference design for the ESS moderators consisted of volume (cylindrical moderators of 16 cm diameter and 13 cm height) parahydrogen moderators, described in the TDR [6, 7]

Low-dimensional moderators of 3 cm height, such as the present butterfly moderator, are expected to deliver a brightness 2.5 times higher the one of the TDR moderators.

Compared to the previous *pancake* design[9], the butterfly moderator offers a significantly higher thermal brightness, and a slightly higher cold brightness, besides the advantages of an easier bi-spectral beam extraction.

The performance of the ESS source is usually compared with the official ILL brightness values from the yellow book [8]. The original design goal of ESS was to achieve a cold peak brightness 30 times the average ILL brightness [6]. With the use of low-dimensional moderators, we are far above this goal. The cold brightness shown in this report is (at 4 Å) nearly 140 times higher than the yellow book value. The thermal brightness at 1.5 Å is about 10 times higher than ILL.¹ Considering integral values, the integrated peak cold brightness above 4 Å for the butterfly is of 4.16×10^{14} n/cm²/s/sr, which is 125 times the ILL average integrated brightness (3.3×10^{12} n/cm²/s/sr). For all cold neutrons above 2 Å, the ESS brightness is of 1.32×10^{15} n/cm²/s/sr, which is 170 times the ILL brightness (7.8×10^{12} n/cm²/s/sr) in the same range. For thermal neutrons, from 0.9 Å to 2 Å, the ESS peak thermal brightness is of 6.25×10^{14} n/cm²/s/sr which is 10 times higher than ILL (6.2×10^{13} n/cm²/s/sr).

¹According to a recent (unpublished) compilation of experimental and computational data, the ILL brightness should be corrected, so that on average the thermal brightness is lower by about a factor of 2, and the cold brightness is on average higher, also by about a factor 2. However, in this report we stick to the comparison with the official yellow book values.

A Method for brightness calculation and optimization

A.1 Detectors

Brightness is calculated for all the beam ports in the two 120° beam extraction openings surrounding the moderators, using point detector f5 tallies placed at 10 m from the moderator surface. The detectors are placed at the 42 angles corresponding to the actual beam port grid.

A.2 Collimators

Fig. 15 shows the viewed horizontal widths at the cold moderator used in the MCNPX model for brightness calculation. The full lines correspond to artificial collimators that look only at the surface defined by the solid lines, at the different angles. In all the calculations the vertical width seen at the moderator surface is always of 3 cm. Concerning horizontal widths, different values at the moderator were considered:

- maximum view width: the brightness is calculated for the maximum viewed surface (Fig. 10 and Table 1)) possible for the thermal and cold moderator.
- 6-cm view width: the ESS moderator were designed having as requirements a 6-cm horizontal width. This is therefore our reference case. In this case the collimators are set as shown in Fig. 15 and Fig. 16.
- 3-cm view width: some instruments will use less than the nominal 6-cm extraction width. It is therefore of great interest to show the maximum brightness achievable by restricting the viewed width to 3 cm. This gives a significant performance increase for some beam lines (see Fig. 13).

A.3 Optimizations

When optimising the guide design for an individual instrument, a two-stage process is recommended. Firstly, the instruments guide should be oriented within the beamport insert to point at the centre the relevant source: for a cold instrument, that is the centre of the circular arc defining the nearest lobe of the hydrogen moderator. For a thermal or bi-spectral instrument, that is the outside surface of the centre of the V shape of the thermal moderator (Fig. 6, bottom). The exact orientation should then be refined using the McStas source component to maximise the instrument performance. The effective brightness of the source will vary by up to about 15% depending on the width and angular acceptance of the guide system.

Fig. 13 shows the impact of changing the horizontal width at the moderator on the moderator brightness, which can give a brightness increase up to 15% for some beam lines. For a given width, the fine tuning of the collimator position can give brightness increases of several %, see for instance Fig. 17 for the thermal moderators. In Appendix A horizontal brightness distribution curves are shown for all the beamports of interest. These indicates that a careful optimization of the optics should be done, with the help of McStas and MCNP calculations, to extract neutrons from the brightest part of the moderator.

A.4 Horizontal brightness distributions at moderator in MCNP and McStas models

In this section we show the horizontal distribution of the brightness at the moderator, for all the relevant beam lines. The beam ports of interest are (list provided by Ken Andersen): W1,

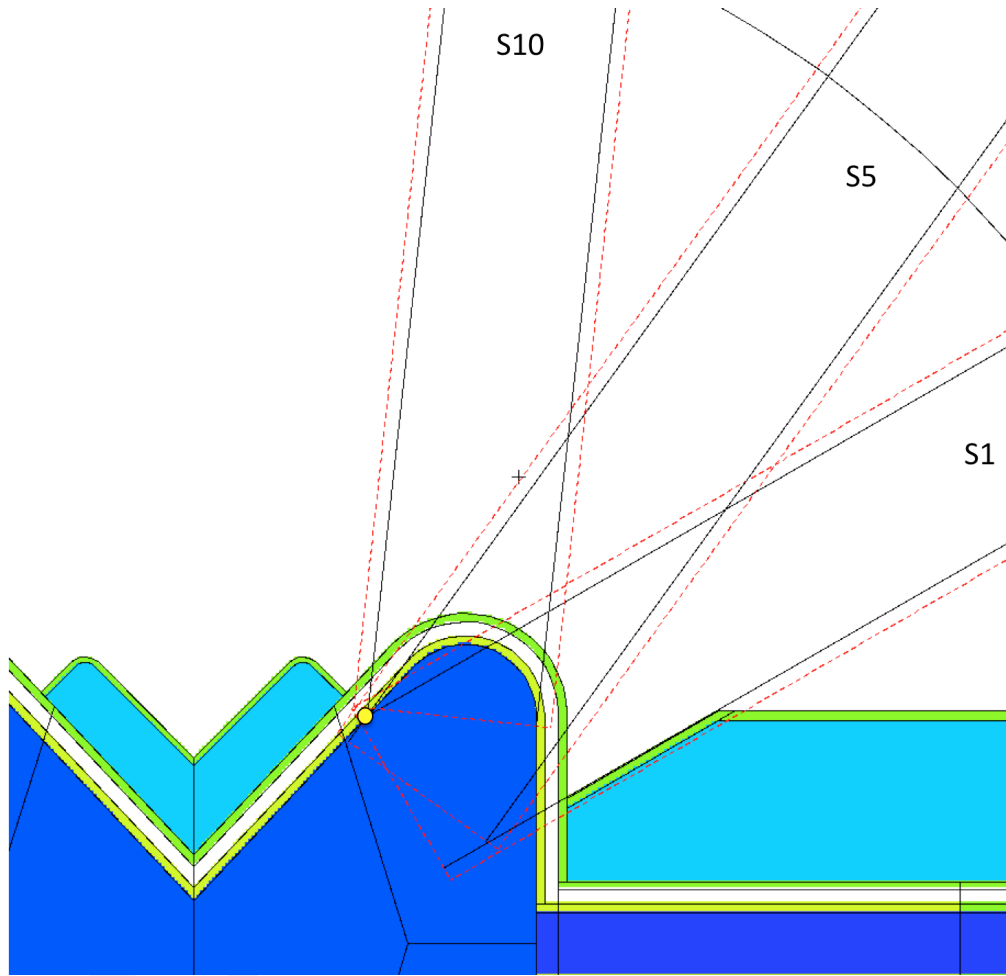


Figure 15: Cold collimators used in the MCNPX model for the brightness calculation. In the figure we show as example the collimators for the S1, S5 and S10 beam lines. The viewed width at the moderator is of 6 cm. All the 42 beam ports are calculated. The collimators view a surface 6 cm wide, 3 cm high.

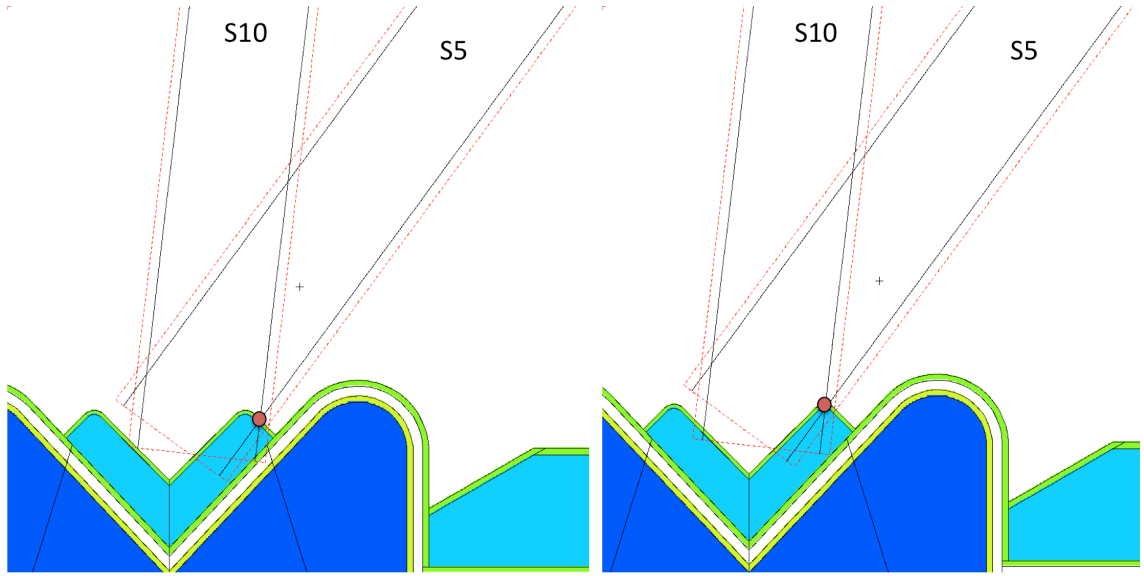


Figure 16: Thermal collimators used in the MCNPX model for the brightness calculation; we show as example the S5 and S10 beam lines. In the two figures the collimators point at slightly different locations of the moderators, passing through the red dots which differ in position by about 1 cm in the two figures. This has an impact on the brightness as shown in Fig. 17, and is an indication as careful optimization of the optics should be done, with the help of McStas and MCNP calculations, to extract neutrons from the brightest part of the moderator.

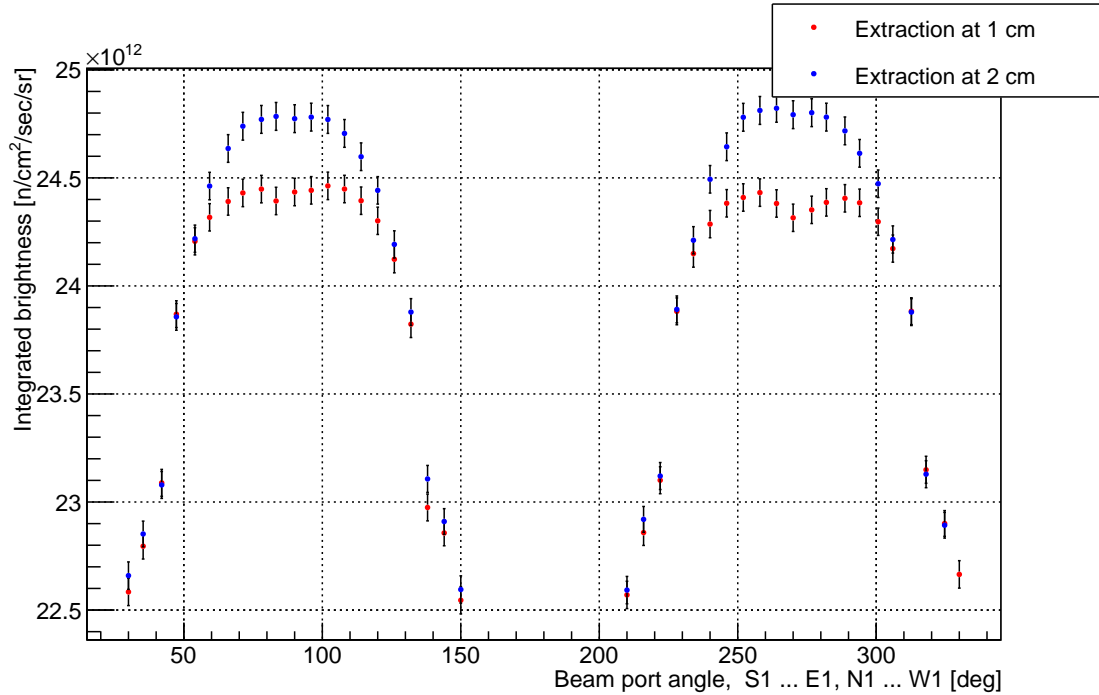


Figure 17: Time average integrated thermal brightness for the 42 beam ports, for different extraction position of thermal neutrons. See Fig. 16 and explanation in the text.

W2, W3, W4, W5, W6, W7, W8, N5, N7, E2, E3, E5, E7, E8, S1, S2, S3, S4. In addition, it is of interest to look at one 90° beam port, possible location for the nnbar experiment. Detailed MCNPX calculations were performed for the following beam ports: E1, W2, W3, W4, W5, W6, W7, W8, and S11. Given the configuration of the beam ports, this covers all the list of interest, since for instance W1 will have the same distribution as E1, N5 and E5 will be like W5, and so on (see Fig. 2).

Calculations were performed with MCNPX using collimators placed at 3 m distance from the moderator, looking at a surface 2 mm wide, 30 mm high, moving the collimator to obtain a distribution across the thermal and cold moderators. Results are shown in Figs. 18 to 27 and compared with the same distributions from the present McStas component (the absolute values of the McStas distributions have been multiplied by a constant factor to compare with the peak brightness units of the MCNPX results. As shown in the figures, overall the agreement between MCNPX and McStas is very good, showing that the present module can be used for guide design. For fine tunings, such as decision of the precise location of the area of neutron extraction, it is however recommended to double check with the MCNPX results, which we could further refine if needed by the instrument design teams.

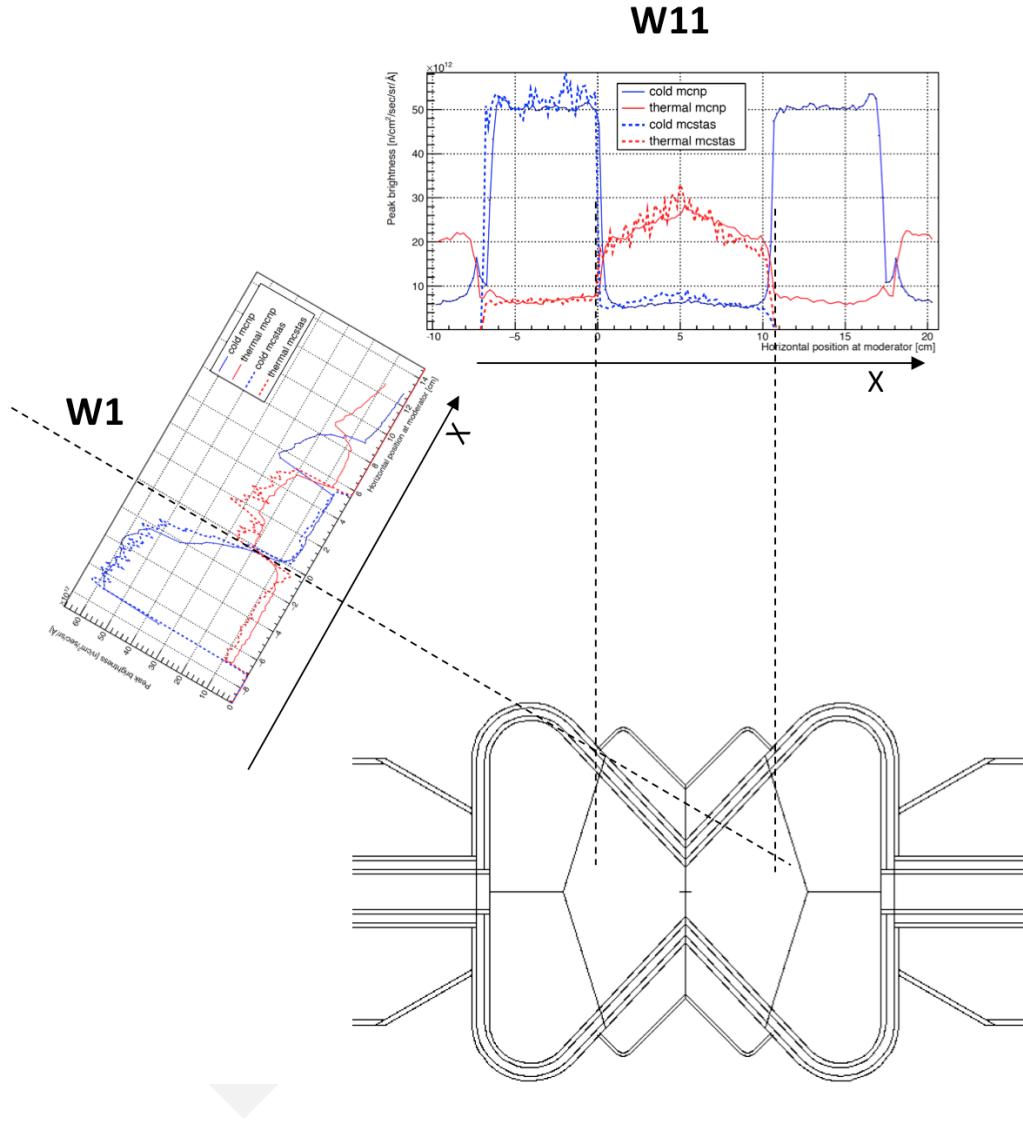


Figure 18: Brightness distribution along an X axis perpendicular to the beam line, shown for W1 and W11 beam ports (the actual calculations were performed for E1 and S11 beam ports, respectively, but the distribution is the same). Dashed lines pass through the focal points and the 0 of the X axis. At 90° (W11) the cold distributions from the two sides of the cold moderator have the same intensity, as expected.

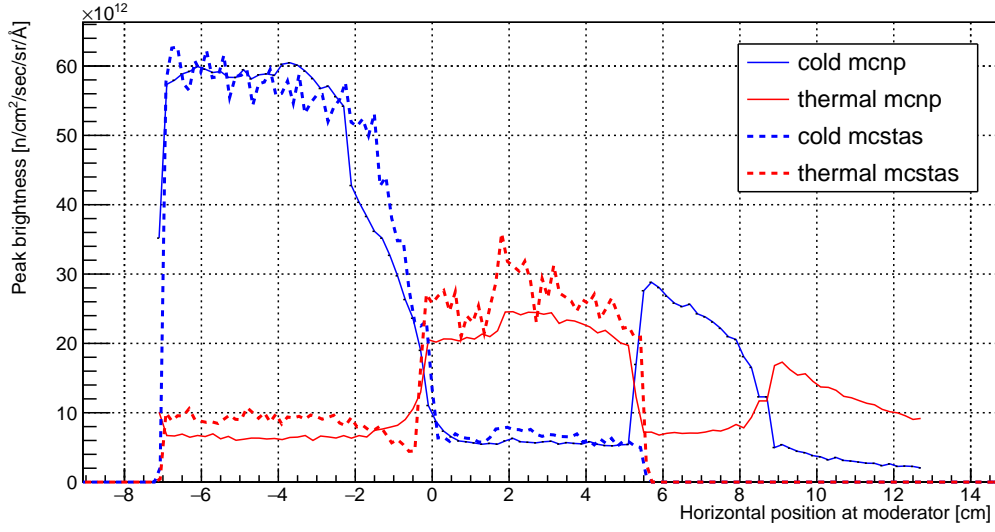


Figure 19: Horizontal brightness distribution for the E1 beam line, for cold ($E < 20$ meV) and thermal ($20 < E < 100$ meV) neutrons. The X axis corresponds to a line perpendicular to the beam port angle, with the 0 corresponding to the focal point (see Fig. 18). The shape of this distribution is also valid for the W1 beam line. Comparison between MCNPX simulations and from the McStas component [1].

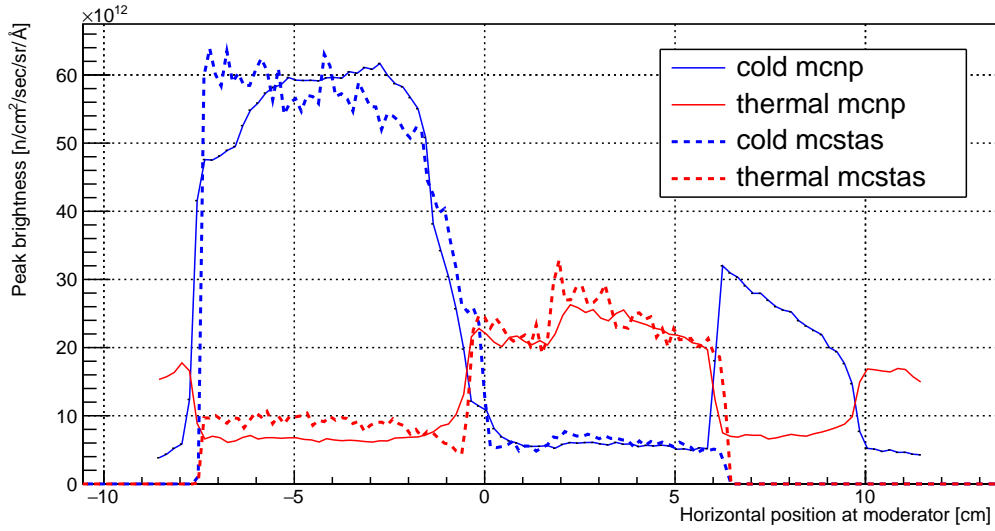


Figure 20: Like Fig. 19 for the W2 beam line. The shape of this distribution is also valid for the E2 and S2 beam lines.

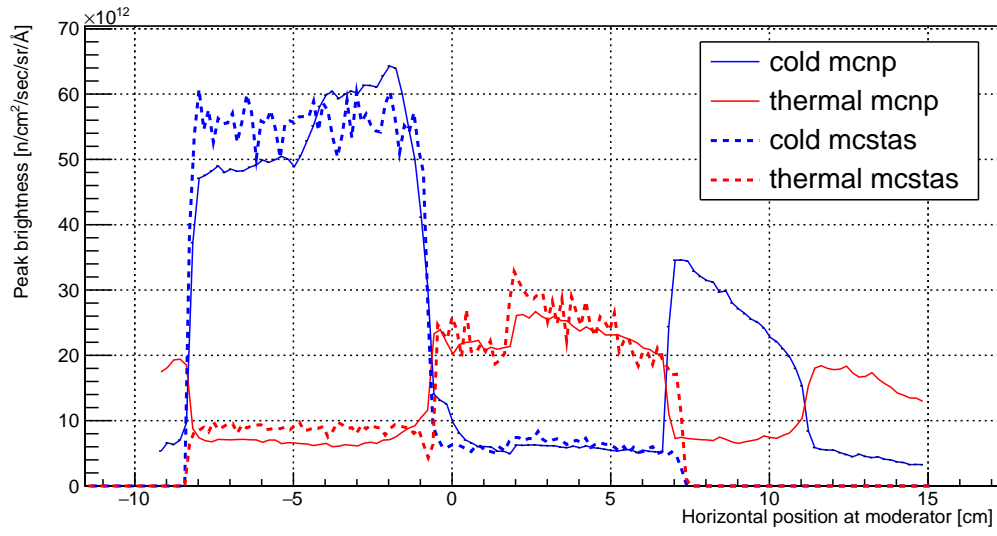


Figure 21: Like Fig. 19 for the W3 beam line. The shape of this distribution is also valid for the E3 and S3 beam lines.

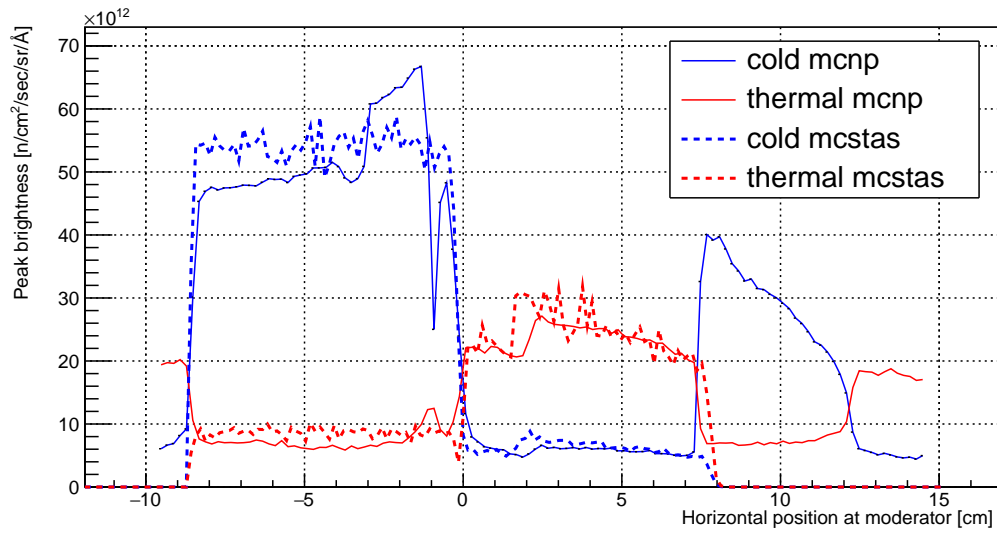


Figure 22: Like Fig. 19 for the W4 beam line. The shape of this distribution is also valid for the S4 beam line.

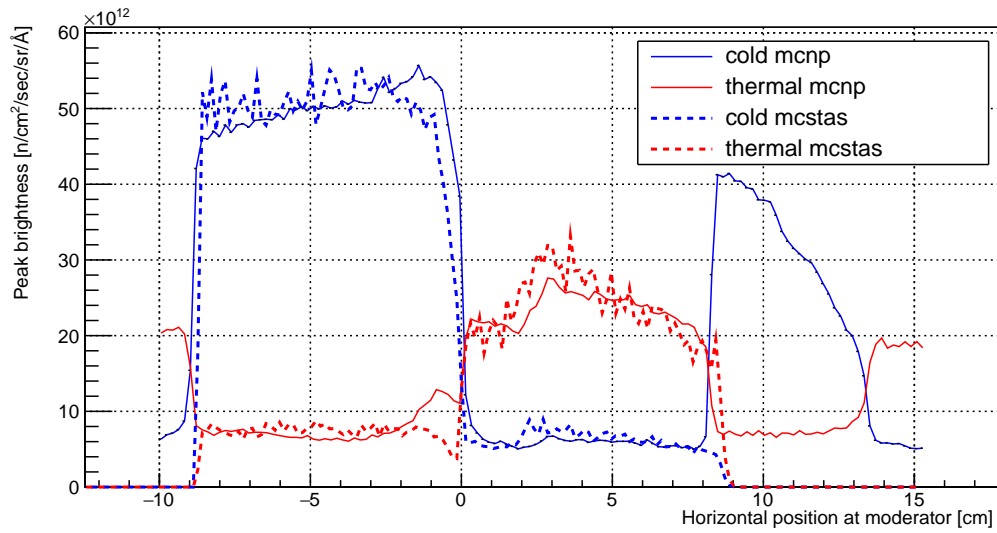


Figure 23: Like Fig. 19 for the W5 beam line. The shape of this distribution is also valid for the N5 and E5 beam lines.

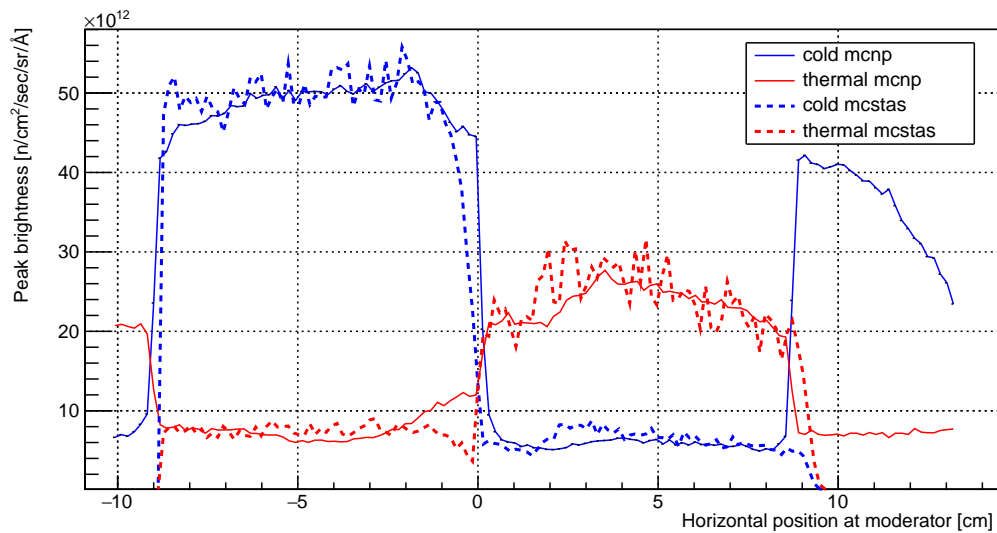


Figure 24: Like Fig. 19 for the W6 beam line.

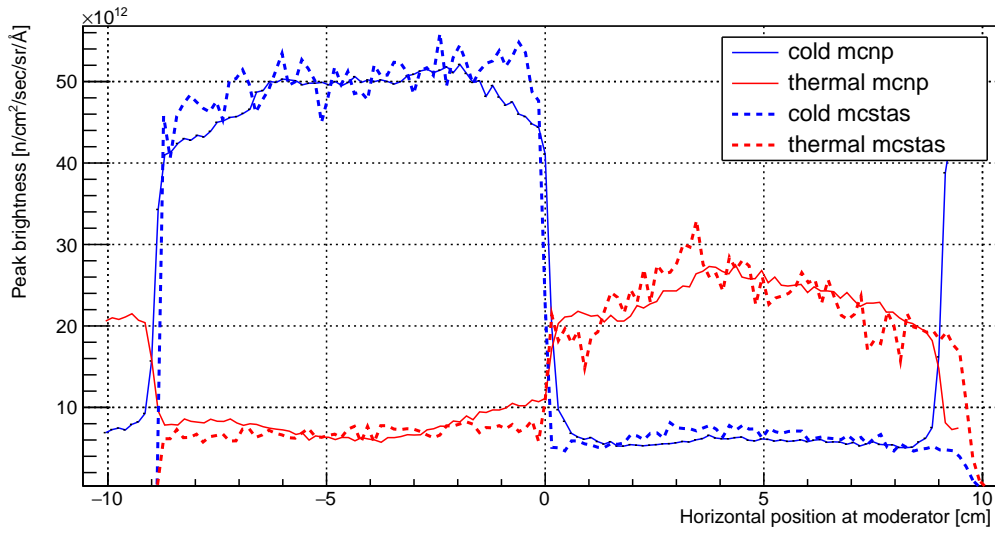


Figure 25: Like Fig. 19 for the W7 beam line. The shape of this distribution is also valid for the N7 beam line.

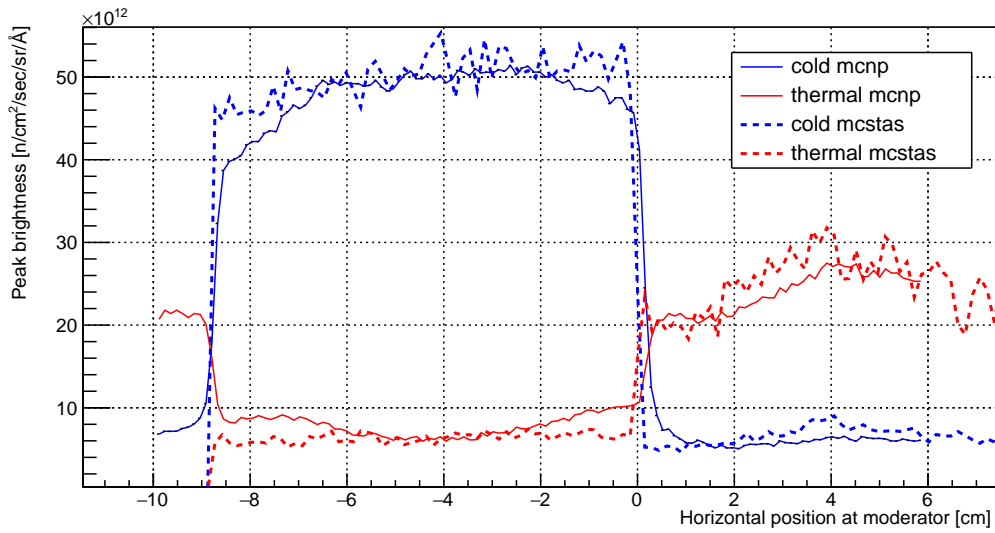


Figure 26: Like Fig. 19 for the W8 beam line. The shape of this distribution is also valid for the E8 beam line.

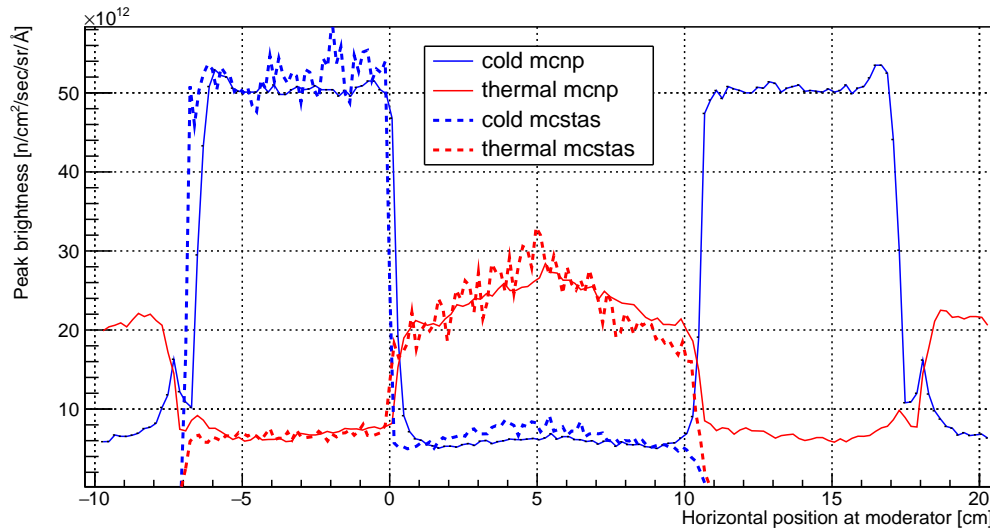


Figure 27: Like Fig. 19 for the S11 beam line. The shape of this distribution is also valid for the W11 beam line.

References

- [1] Ken Andersen, Peter Willendrup, Luca Zanini, Update to ESS moderators.
- [2] L. Zanini, K. Batkov, F. Mezei, A. Takibayev, E. Klinkby, T. Schönfeldt, *The neutron moderators at the European Spallation Source*, proceedings of the AccApp15 conference, in course of publication.
- [3] T. Schönfeldt, *Advanced Neutron Moderators*, PhD thesis, Danish Technical University, 2016.
- [4] K. Batkov, A. Takibayev, L. Zanini and F. Mezei, Unperturbed moderator brightness in pulsed neutron sources, *Nuclear Instruments and Methods in Physics Research Section A: Accelerators, Spectrometers, Detectors and Associated Equipment* 729 (2013) 500 - 505. doi:<http://dx.doi.org/10.1016/j.nima.2013.07.031>.
- [5] F. Mezei, L. Zanini, A. Takibayev, K. Batkov, E. Klinkby, E. Pitcher, and T. Schönfeldt, Low dimensional neutron moderators for enhanced source brightness, *Journal of Neutron Research* 17 (2014) 101105.
- [6] ESS Technical Design Report, S. Peggs editor, ISBN 978-91-980173-2-8, 2013, <http://europeanspallationsource.se/scientific-technological-documentation>
- [7] M. Magán et al., Neutronic analysis of the bi-spectral moderator such as that proposed for ESS *Nucl. Instrum. Methods A* 729 (2013) 417425.
- [8] Institut Laue-Langevin. 'ILL Yellow Book 2008.' <http://www.ill.eu/?id=1379>, 2008.
- [9] L. Zanini, K. Batkov, E. Klinkby, F. Mezei, E. Pitcher, T. Schnfeldt, A. Takibayev, Moderator configuration options for ESS, *Proceedings of the ICANS XXI conference*, Mito, Japan, 2014.
- [10] Waters L. S. et al. 2007. The MCNPX Monte Carlo radiation transport code. *AIP Conf.Proc.* **896**, 81-90.

- [11] D. Pelowitz, editor, MCNPX Users Manual, Version 2.7.0, Number LA-CP-11-0438, 2011.
- [12] L. B. Grammer et al., Measurement of the scattering cross section of slow neutrons on liquid parahydrogen from neutron transmission, Phys. Rev. B 91, 180301(R) (2015).
- [13] L. Zanini, *Request for baseline change: TS.BASELINE.V2.CHANGE.002*, ESS internal document, 8 June 2012.